Non-invasive Blood-Glucose Estimation Using Smartphone PPG Signals and Subspace KNN Classifier

Yuwei Zhang[1]**, Yuan Zhang**[1,†]**, Sarah Ali Siddiqui**[1]**, Anton Kos**[2]

[1]*Shandong Provincial Key Laboratory of Network Based Intelligent Computing, University of Jinan, Jinan, China*
[2]*Faculty of Electrical Engineering, University of Ljubljana, Ljubljana, Slovenia*
[†] *E-mail: yzhang@ujn.edu.cn*

Abstract. Non-invasive healthcare monitoring systems based on machine learning and wearable sensors hold the future of smart health. Ubiquitous use of smartphones makes them an excellent choice for designing or developing cost-effective and portable smart health monitoring systems. A non-invasive blood-glucose estimation system is proposed that utilizes a smartphone camera for data acquisition and generates an output using a machine-learning algorithm. The focus of the system is to (1) acquire PPG signals using a smartphone, (2) classify valid and invalid signals, (3) estimate the blood-glucose levels from the valid signals by applying a subspace KNN classifier. The system requires no re-calibration or individually dependent calibration. Its overall training accuracy is 86.2% and the accuracy of the invalid single-period classification is 98.2%.

Keywords: Non-invasive blood-glucose estimation, Smartphone, Photoplethysmography (PPG), Healthcare based on machine learning, Subspace KNN classifier

Neinvazivna metoda ocenjevanja ravni krvnega sladkorja s pomočjo PPG na pametnem telefonu in podprostorske KNN

Prihodnost zdravstvenih sistemov je v neinvazivnih sistemih za spremljanje zdravja na osnovi nosljivih senzorjev in strojnega učenja. Vseprisotna uporaba pametnih telefonov je odlična priložnost za načrtovanje in razvoj prenosnih in stroškovno učinkovitih pametnih sistemov za spremljanje zdravja. Predlagamo neinvazivno metodo ocenjevanja ravni krvnega sladkorja, ki za pridobivanje podatkov uporablja kamero pametnega telefona in podaja rezultate na osnovi strojnega učenja. Poudarek članka je na: (1) pridobivanju fotopletizmografičnih (PPG) signalov s pametnim telefonom, (2) razvrščanju signalov v veljavne in neveljavne, (3) oceno ravni krvnega sladkorja z uporabo podprostorskega klasifikatorja KNN. Predlagani sistem ne zahteva ponovne kalibracije ali kalibracije v odvisnosti od posameznika. Njegova skupna natančnost dosega 86,2%, natančnosti klasifikacije veljavnosti period signalov pa 98,2%.

1 INTRODUCTION

Diabetes is one of the most widely spread chronic illnesses/diseases caused by imbalance in glucose concentration in the body. This instability can lead to serious problems, e.g. cardiovascular diseases, kidney failure,

blindness, etc. [1]. It is expected that by 2030, diabetes will use up to 11.6% of the total expenses made in the healthcare domain [2]. Hyperglycemia is a condition in which the glucose level is higher than 180 mg/dl, whereas hypoglycemia is a condition caused by a very low glucose level, i.e. lower than 70 mg/dl [3], [4]. There is no cure for diabetes so far but monitoring under the glucose level regularly helps in keeping diabetes in control [5], [6], [7]. Self monitoring is one of the most feasible and helpful/useful solutions to control diabetes.

As explained in our recent work [8], glucose monitoring can be grouped into invasive, minimally invasive and non-invasive. Conventional glucose monitoring requires a blood sample by pricking the fingertip of the patient with a needle/lancet making frequent monitoring inconvenient, painful, uncomfortable and costly for the users [9], [10]. Non-invasive glucose monitoring is the focus of the current and future research since it is pain-free, risk-free, convenient and comfortable for users [11]. Artificial intelligence and expert systems are being used in order to make such monitoring systems accurate and efficient [12], [13].

Photoplethysmographic (PPG) signals are widely used physiological signals for basic vitals monitoring [14]. Light is illuminated on a certain part of the body. A part of that light is absorbed by the body and the other part is reflected back. The amount of the reflected light varies with the varying amount of blood flowing through that body part and can be used to acquire the PPG signals

[15]. Conventionally, the PPG signals are obtained by using wearable pulse oximeters on different parts of the human body, e.g. fingertip, ear, wrist, etc. [16].

Wearable sensors with the support of smartphones can be used to track the basic vitals. They acquire the data from the body and smartphones process the data [17], [18]. Instead of using these two components separately, we combine them by using a smartphone camera for data acquisition. The smartphone camera with its LED on captures a video of the fingertip that is used to extract the PPG signals.

As mentioned earlier, machine learning is being extensively used in the healthcare domain for analyzing clinical data, estimating basic human vitals and managing diseases, etc. [19], [20]. In our system, the blood-glucose levels are estimated by using a machine-learning algorithm for the PPG signals acquired by using a smartphone camera. To the best of our knowledge, the existing works do not make use of machine-learning approaches to classify the valid and invalid PPG signals, while in our work we first separate the invalid data from the valid signals and them classify valid signals into two blood-glucose groups. To acquire the PPG signals, the existing systems utilize a certain hardware, e.g. a finger clip and laser light, whereas our system uses only smartphone needing no individually-based calibration. With this very convenient and non-invasive system, a user can learn if his/her blood-glucose level does not fall into a normal group. Then he/she can further get on exact value using an invasive method. Our system monitor on improved accuracy with the smallest possible number of features. Its main contributions on:

- Designed and developed cost-effective non-invasive blood-glucose estimation system is of a high accuracy and robustness.

- The used machine-learning classification algorithms differentiate between the valid and invalid PPG signals.

- The used machine-learning classification algorithms classify the valid signals into two blood-glucose groups.

- The system effectiveness is proven by comprehensive and solid experimental validation.

The rest of the paper is organized as follows. Section 2 describes the proposed system. The results obtained using the proposed system are explained in section 3. Section 4 provides a discussion. Section 5 concludes the paper.

2 DESCRIPTION OF THE PROPOSED SYSTEM

To estimate the blood-glucose groups non-invasively, the system uses smartphone PPG signals combined with

Table 1. Blood-glucose groups

Groups	Blood Glucose Ranges (mg/dl)
G1	70-100
G2	101-130
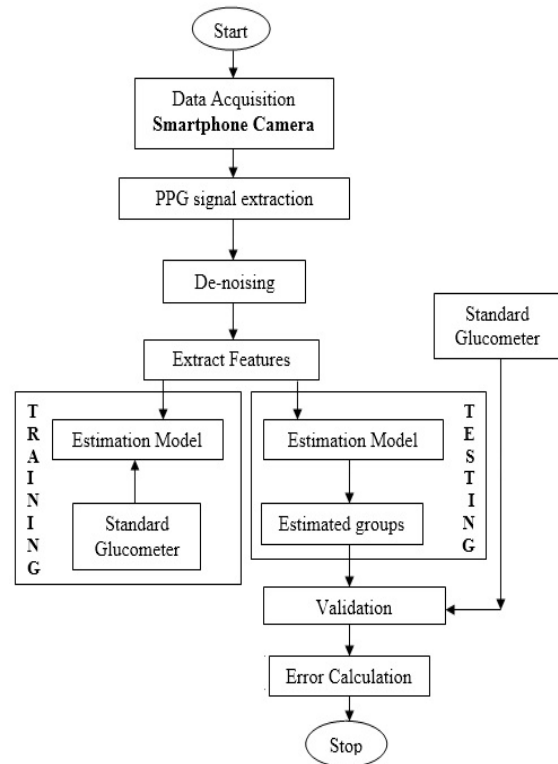
Figure 1. Flowchart of the proposed system.

machine-learning algorithms, such as Bagged Trees, RUS Boosted Trees, Subspace KNN and Decision Trees. A flowchart of the proposed system is shown in Fig. 1. The blood-glucose scale level from 70-130 mg/dl is divided into two groups shown in Table 1. The system classifies the PPG data from the smartphone into three groups, i.e. a group of invalid data (G0) and two groups of valid data (G1 and G2).

2.1 Signal Acquisition

A smartphone camera with a frame rate of 28 fps (sampling rate 28 Hz) is used to record a 30-40 seconds long video of the left hand index finger. During the recording phase, the fingertip covers both the flash and the camera. The reflection-mode PPG signals are acquired from the recorded videos (Fig. 3) [21]. At the same time, the glucose levels from a standard glucometer are recorded for labeling (two groups). The video is then transferred to a computer for processing in MATLAB. Red, green and blue channels are extracted from individual frames of the video. The threshold is set using Eq. 1 of our previous work where we designed a
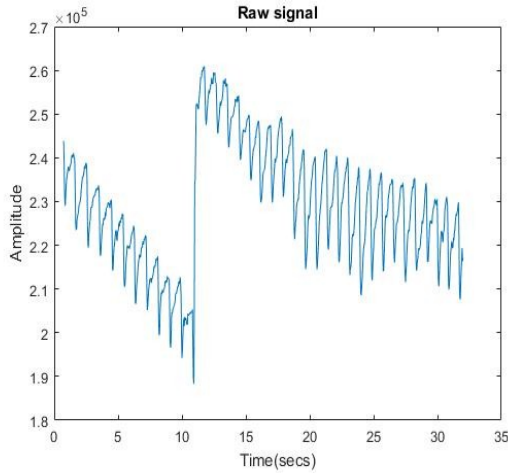
Figure 2. Raw smartphone PPG signal.
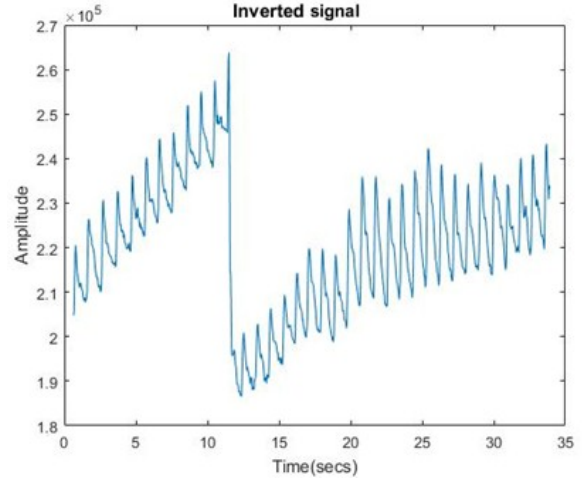
Figure 3. Inverted smartphone PPG signal.

PPG-based algorithm for the heart rate estimation [21]. The pixels having an intensity greater than the defined threshold are summed up normally for each frame using Eq. 2 [21]. The PPG signal is obtained by plotting the calculated sum of each frame.

14 volunteering subjects were asked to keep their hands steady while video-recording and about 850 samples were collected for each subject. The age of the subjects from 20-33 years and the glucose level range of them was from 70-130 mg/dl. This glucose level range was selected after a thorough experimentation using a PPG signal acquisition lab-built device. A device showed the best classification results were obtained for the glucose level range from 70-130 mg/dl.

2.2 Signal Preprocessing

The reflection-mode PPG signals are extracted from the recorded videos for each subject using the system involved in Section 3.1. The acquired raw signals are inverted because of the reflection mode shown in Figs. 2 and 3, respectively. The PPG signals are prone to the noise and motion artifacts, so the inverted signals are de-noised using a Butterworth filter to remove the frequency components higher than 12 Hz as shown in Fig. 4.

After de-noising, the baseline wander is removed to bring the signal back to its normal base (x-axis). A resulted signal is shown in Fig. 5. A signal is then segmented into single periods, i.e. one complete PPG cycle using on iterative sliding-window (ISW) algorithm proposed in our paper [22].

2.3 Feature Extraction

The time-domain waveform (PPG) and its first derivative (VPG) and second derivative (APG) are utilized for feature extraction. 439 single periods obtained with segmentation are in section IIIB labeled as G0, invalid, or G1-G2, valid as described in Table I. The valid and invalid single-period examples are shown in Figs. 6
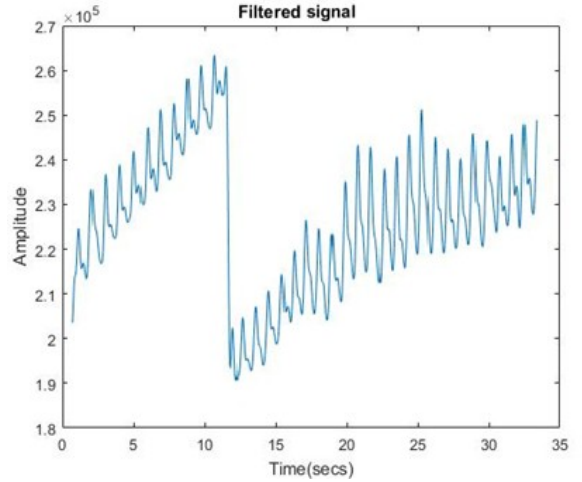
Figure 4. Filtered smartphone PPG signal.
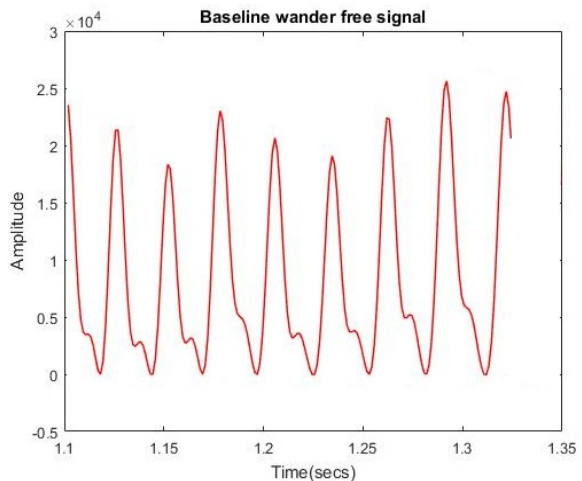
Figure 5. PPG signal after baseline wander removal.

and 7, respectively. 26 features are then extracted from the time-domain waveform shape of each period, 11

Table 2. Extracted features from the smartphone PPG signals

Feature	Definition
width_period	The time taken for one period
highest_peak_value	The maximum amplitude of the signal
time_highest_peak	The value of the time when the amplitude is maximum
peaks_first_seg	The number of the peaks from the start to the peak
dis_peak	The amplitude of the diastolic peak
time_distolicpeak	The value of the time when the diastolic peak occurs
notch	The amplitude of the notch
time_notch	The value of the time when the notch occurs
range_values	The range of the amplitude values in a single period
slope_rise	The rising rate of the single period from the start to the peak
slope_fall	The falling rate of the single period from the peak to the end
timediff_start_peak	The total time taken from the start to the peak
timediff_peak_notch	The total time taken from the peak to the notch
timediff_notch_distolicpeak	The total time taken from the notch to the diastolic peak
timediff_distolicpeak_end	The total time taken from the diastolic peak to the end
mean_value_single	The mean amplitude value of the single period
number_values	The length of the single period
Standard_deviation	The standard deviation of the amplitudes
mean_start_max	The mean amplitude from the start to the peak
mean_max_notch	The mean amplitude from the peak to the notch
mean_notch_distolicpeak	The mean amplitude from the notch to the diastolic peak
mean_distolicpeak_end	The mean amplitude from the diastolic peak to the end
meanslope_sp	The mean slope from the start to the peak
meanslope_pn	The mean slope from the peak to the notch
meanslope_nd	The mean slope from the notch to the diastolic peak
meanslope_de	The mean slope from the diastolic peak to the end
max_deriv1	The maximum amplitude of the first derivative
time_max_deriv1	The value of the time when the amplitude of the first derivative is maximum
lowpeak_deriv1	The amplitude of the second highest peak of the first derivative
lowpeak_deriv1_time	The value of the time when the second highest peak of the first derivative occurs
diff_d1peaks_value	The difference in the amplitude of a maximum and second highest peak of the first derivative
diff_d1peaks_time	The time taken from the maximum to the second highest peak of the first derivative
valley1_derv1_value	The amplitude of the first valley of the first derivative
valley2_derv1_value	The amplitude of the second valley of the first derivative
valley1_derv1_time	The value of the time when the first valley of the first derivative occurs
valley2_derv1_time	The value of the time when second valley of the first derivative occurs
diff_valleytime_derv1	The time taken from the first to the second valley of the first derivative
max_deriv2	The maximum amplitude of the second derivative
time_max_deriv2	The value of the time when the amplitude of the second derivative is maximum
lowpeak_deriv2	The amplitude of the second highest peak of the second derivative
lowpeak_deriv2_time	The value of the time when the second highest peak of the second derivative occurs
diff_d2peaks_value	The difference in amplitude of maximum and the second highest peak of the second derivative
diff_d2peaks_time	The time taken from maximum to the second highest peak of the second derivative
valley1_derv2_value	The amplitude of the first valley of the second derivative
valley2_derv2_value	The amplitude of the second valley of the second derivative
valley1_derv2_time	The value of the time when the first valley of the second derivative occurs
valley2_derv2_time	The value of the time when the second valley of the second derivative occurs
diff_valleytime_derv2	The time taken from the first to the second valley of the second derivative
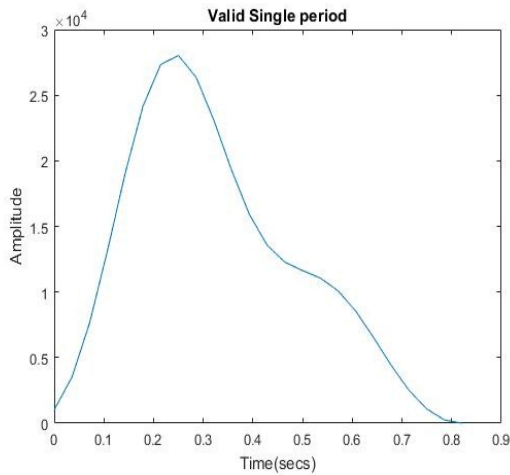
Figure 6. Valid smartphone single period.
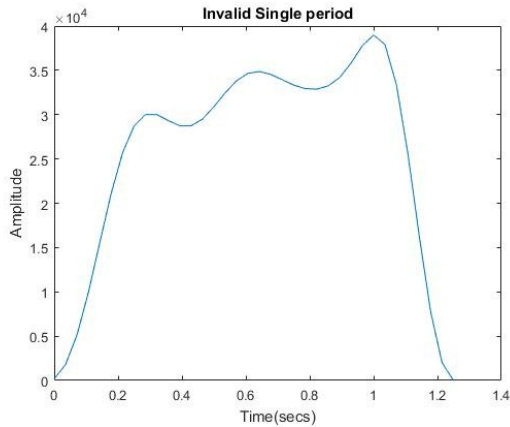
Figure 7. Invalid smartphone single period.

features from its first derivative and 11 from its second derivative as shown in Table 2. The first 19 values of the time-domain PPG signal are used as additional features making the total number of features 67. The feature values for each single period are then acquired to make a feature-matrix having 439 rows, each representing a single period, and columns representing different features, labels and the number of the subject. In Figures 2-7, the amplitude on the vertical axis represents the sum of the pixels having the intensity greater than the threshold.

2.4 Classification (training and testing datasets)

The feature-matrix for the dataset (439 single periods) is randomly divided into a training (217 single periods) and testing (221 single periods) dataset randomly. Due to the small number of the volunteering subjects, the 439 single periods are considered as 439 unique signals out of which 217 single periods are used to train the classification models (Bagged Trees, RUS Boosted Trees, Decision Trees and Subspace KNN) and the remaining 221 single periods are used for validating

the classification accuracy. The labels assigned to the training dataset for the invalid (G0) and valid (G1 and G2) are classification (0, 1 and 2), respectively. The classification used are Bagged Trees, RUS Boosted Trees, Decision Trees and Subspace KNN. A five-fold cross-validation of a single period is performed.

3 RESULTS

The dataset selected for this experiment is kept between the glucose level from 70-130 mg/dl. The PPG signals acquired from different subjects are segmented into single periods each considered as a unique signal. Four different classifiers are used, i.e. the Subspace KNN, RUS boosted trees, Bagged trees and Decision trees. The accuracy is over 80% for the G0, G1 and G2 classification made with the Subspace KNN classifier at a high 86.2% which is marginally higher than with the Bagged trees, whereas for on invalid single-period classification, the Subspace KNN classifier out-performes all the other classifiers with an accuracy of 98.2% which is only about a percentage point higher than with the Bagged trees with 96.7%. The lowest accuracy is observed with the Decision trees. A comparison between different classifiers is presented in Table 3.

In the group-based classification (G1 and G2) using the Subspace KNN classifier, three out of fourteen subjects (numbered 9, 13 and 14) are classified incorrectly as shown in Table 4. Our detailed experimental results for the G1 and G2 group classification are presented in Table 4.

Table 3. Comparison between different classifiers

Classifier	Overall accuracy	Invalid sample classification
Subspace KNN	86.2%	98.2%
RUS Boosted Trees	85%	90.2%
Bagged Trees	86%	96.7%
Decision Trees	80.1%	83.6%

Table 4. Results for the G1 and G2 classification

No.	Actual group	Estimated group
1.	G1	G1
2.	G2	G2
3.	G1	G1
4.	G1	G1
5.	G2	G2
6.	G2	G2
7.	G2	G2
8.	G1	G1
9.	G2	G1
10.	G1	G1
11.	G2	G2
12.	G2	G2
13.	G2	G1
14.	G1	G2

4 DISCUSSION

To the best of our knowledge, the existing works do not differentiate between the valid and invalid PPG blood-glucose signals. Using our system, the invalid data (G0) are separated from the valid signals and then classified as valid signals of the G1 or G2 group. A brief summary of the existing works on the topic is as follows:

In [18], a blood-glucose and blood-pressure estimation system is proposed utilizing the effect of physiological variations, such as blood viscosity, vessel compliance, heart rate and breathing rate, etc., on the PPG signal waveform. PPG signal is acquired using a finger clip. It is de-noised to remove motion artifacts and then the features are extracted to be fed to different classifiers, e.g. neural networks (NN), linear regression, random forest and SVM. The random forest outperforms the other machine-learning techniques. Using the Clarke Grid Analysis (CGA), 87.7% points are found to fall into region A.

In [2], the PPG signals acquired by a finger clip are used to estimate the blood-glucose levels based on the difference in the optical densities. The acquired signals are converted to electric signals, filtered for noise removal using a series of filters to get the PPG signals. The PPG signals are then filtered using an adaptive neural-network filter to remove motion artifacts and the glucose levels are predicted using artificial neural networks for Field Programmable Gate Arrays (FPGA). The data is collected from 50 subjects for three different wavelengths. The model is trained and tested using a MATLAB toolbox for neural networks and the estimation accuracy is 95.38%.

In [23], the data is acquired by capturing the laser light transmitted by a fingertip with a smartphone camera. An application is developed to extract the intensity of the RGB pixels from every frame. The glucose level is determined by using the blue and green component intensities in the modified Beer-Lambert law and the glucose level measured by a smartphone is linearly proportional to the actual glucose level. The experimental results are calculated using MATLAB for both the glucose solution and blood. The glucose levels are examined 15 and 45 minutes after drinking cola.

The existing systems use a specific hardware, e.g. a finger clip and laser light, to acquire the PPG signals, whereas our system uses only a smartphone to acquire the PPG signals with no need for an individually-based calibration, making this solution very convenient and cost-effective for users. With this non-invasive method, a user can check if his/her blood-glucose value falls into a normal group or not. Then he/she can get the exact value using an invasive method. The proposed system yields an improved accuracy with the smallest possible number of features.

Our study shows that the PPG signals contain on adequate information regarding the blood-glucose level. As observed in [23], changes in the blood-glucose level affect the PPG signals. The results show that after sugar intake, the PPG signals change.

In our previous study [21], the PPG signals acquired from a smartphone camera are utilized to calculate the heartrate of an individual. In the current study, the same procedure is used to acquire the PPG signals from different subjects to classify them into two subnormal blood glucose-groups, G1 and G2.

Machine-learning algorithms distinguish between the valid and invalid PPG signals with an absolute accuracy. The valid signals are classified into two blood-glucose subnormal groups using machine-learning algorithms with a considerably high accuracy.

Each of the four machine-learning algorithms, i.e. the Subspace KNN, RUS boosted trees, Bagged trees and Decision trees, provide an acceptable classification result which shows that the PPG signals can indicate the blood-glucose level.

5 CONCLUSION & FUTURE WORK

The PPG signals are acquired using only a smartphone camera. The blood-glucose level is estimated by denoising and removing the baseline wander, and segmenting the acquired PPG signals into single periods. 67 features are then extracted from the shape of a single period, its first and second derivative signals. The two blood-glucose groups are G1 (70-100 mg/dl) and G2 (101-130 mg/dl). G0 is a group of invalid single periods. The accuracy of the invalid single-period classification and the overall classification result are 98.2% and 86.2%, respectively. Using a smartphone makes the system cost-effective, portable and easy to use.

This work is still at its preliminary stage with only two blood-glucose groups classified and a limited number of subjects. Our future goal is to utilize a larger dataset with a wider range of the age and a higher blood-glucose level. The blood-glucose groups will be reduced and eventually a model will be designed for a specific blood-glucose value estimation. The accuracy for other groups will be improved with the smallest possible error, processing time and energy. With on accuracy note applicable for clinical medicine, a smartphone application with the developed enabling transmission of the data to a computer, storing the results for future reference, alerting/warning, and monitoring spoken instructions and results.

REFERENCES

[1] R. Periyasamy and S. Anand, "A study on non-invasive blood glucose estimation; an approach using capacitance measurement technique," in *2016 International Conference on Signal Processing, Communication, Power and Embedded System (SCOPES)*, Oct 2016, pp. 847–850.

[2] S. Ramasahayam, L. Arora, S. R. Chowdhury, and M. Anumukonda, "Fpga based system for blood glucose sensing using photoplethysmography and online motion artifact correction using adaline," in *2015 9th International Conference on Sensing Technology (ICST)*. IEEE, 2015, pp. 22–27.

[3] L. L. Nguyen, S. Su, and H. T. Nguyen, "Neural network approach for non-invasive detection of hyperglycemia using electrocardiographic signals," in *2014 36th Annual International Conference of the IEEE Engineering in Medicine and Biology Society*, Aug 2014, pp. 4475–4478.

[4] G. Kriukova, N. Shvai, and S. V. Pereverzyev, "Application of regularized ranking and collaborative filtering in predictive alarm algorithm for nocturnal hypoglycemia prevention," in *2017 9th IEEE International Conference on Intelligent Data Acquisition and Advanced Computing Systems: Technology and Applications (IDAACS)*, vol. 2, Sept 2017, pp. 634–638.

[5] L. L. Nguyen, S. Su, and H. T. Nguyen, "Neural network approach for non-invasive detection of hyperglycemia using electrocardiographic signals." IEEE, 2014, pp. 4475–4478.

[6] J. Yadav, A. Rani, V. Singh, and B. M. Murari, "Prospects and limitations of non-invasive blood glucose monitoring using near-infrared spectroscopy," *Biomedical signal processing and control*, vol. 18, pp. 214–227, 2015.

[7] J. Shin, H. Park, S. Cho, H. Nam, and K. J. Lee, "A correction method using a support vector machine to minimize hematocrit interference in blood glucose measurements." *Computers in Biology & Medicine*, vol. 52, no. 3, pp. 111–118, 2014.

[8] S. A. Siddiqui, Y. Zhang, J. Lloret, H. Song, and Z. Obradovic, "Pain-free blood glucose monitoring using wearable sensors: Recent advancements and future prospects," *IEEE Reviews in Biomedical Engineering*, pp. 1–1, 2018.

[9] A. K. Seifert, N. Demitri, and A. M. Zoubir, "Decreasing the measurement time of blood sugar tests using particle filtering," in *ICASSP*, 2016.

[10] N. Demitri and A. Zoubir, "Measuring blood glucose concentrations in photometric glucometers requiring very small sample volumes." *IEEE transactions on bio-medical engineering*, 2016.

[11] C. A. Jung and S. J. Lee, "Design of automatic insulin injection system with continuous glucose monitoring (cgm) signals," in *2016 IEEE-EMBS International Conference on Biomedical and Health Informatics (BHI)*, Feb 2016, pp. 102–105.

[12] A. K. Tripathy, R. Carvalho, K. Pawaskar, S. Yadav, and V. Yadav, "Mobile based healthcare management using artificial intelligence," in *2015 International Conference on Technologies for Sustainable Development (ICTSD)*, Feb 2015, pp. 1–6.

[13] M. Chen, X. Shi, Y. Zhang, D. Wu, and M. Guizani, "Deep features learning for medical image analysis with convolutional autoencoder neural network," *IEEE Transactions on Big Data*, vol. PP, no. 99, pp. 1–1, 2017.

[14] A. Hernando, M. D. Peláez, M. T. Lozano, M. Aiger, E. Gil, and J. Lázaro, "Finger and forehead ppg signal comparison for respiratory rate estimation based on pulse amplitude variability," in *2017 25th European Signal Processing Conference (EUSIPCO)*, Aug 2017, pp. 2076–2080.

[15] K. T. Tanweer, S. R. Hasan, and A. M. Kamboh, "Motion artifact reduction from ppg signals during intense exercise using filtered x-lms," in *2017 IEEE International Symposium on Circuits and Systems (ISCAS)*, May 2017, pp. 1–4.

[16] C. Choi, B. H. Ko, J. Lee, S. K. Yoon, U. Kwon, S. J. Kim, and Y. Kim, "Ppg pulse direction determination algorithm for ppg waveform inversion by wrist rotation," in *2017 39th Annual International Conference of the IEEE Engineering in Medicine and Biology Society (EMBC)*, July 2017, pp. 4090–4093.

[17] M. Jagelka, M. Donoval, P. Telek, F. Horǎnek, M. Weis, and M. DaĹ™ÄÄŤek, "Wearable healthcare electronics for 24-7 monitoring with focus on user comfort," in *2016 26th International Conference Radioelektronika (RADIOELEKTRONIKA)*, April 2016, pp. 5–9.

[18] E. Montemoreno, "Non-invasive estimate of blood glucose and blood pressure from a photoplethysmograph by means of machine learning techniques." *Artificial Intelligence in Medicine*, vol. 53, no. 2, pp. 127–138, 2011.

[19] R. Bhardwaj, A. R. Nambiar, and D. Dutta, "A study of machine learning in healthcare," in *2017 IEEE 41st Annual Computer Software and Applications Conference (COMPSAC)*, vol. 2, July 2017, pp. 236–241.

[20] H. Geng, *Data Analysis and Machine Learning Effort in Healthcare*. Wiley Telecom, 2017, p. 816. [Online]. Available: https://onlinelibrary.wiley.com/doi/pdf/10.1002/9781119173601.ch18

[21] S. A. Siddiqui, Y. Zhang, Z. Feng, and A. Kos, "A pulse rate estimation algorithm using ppg and smartphone camera," *Journal of medical systems*, vol. 40, no. 5, pp. 1–6, 2016.

[22] Z. Zhang, Y. Zhang, L. Yao, H. Song, and A. Kos, "A sensor-based wrist pulse signal processing and lung cancer recognition," *Journal of Biomedical Informatics*, vol. 79, pp. 107–116, Mar 2018.

[23] V. Dantu, J. Vempati, and S. Srivilliputhur, "Non-invasive blood glucose monitor based on spectroscopy using a smartphone," in *2014 36th Annual International Conference of the IEEE Engineering in Medicine and Biology Society*. IEEE, 2014, pp. 3695–3698.

Yuwei Zhang received her B.Sc in Communication Engineering in 2016 from University of Jinan, China. She is a master student majoring in computer science at Shandong Provincial Key Laboratory of Network-Based Intelligent Computing, University of Jinan. She is a member of ACM and CCF. Her current research interests include biomedical signal/image processing machine learning and pattern recognition.

Yuan Zhang received his M.Sc. degree in communication systems and the Ph.D. degree in control theory and engineering (Biomedical Engineering) from Shandong University, China, in 2003 and 2012, respectively. He is currently a Professor with the University of Jinan, China. As the first author or corresponding author he has published more than 50 peer reviewed papers in international journals and conference proceedings, a book chapter, and six patents in the areas of Smart Health and Biomedical Big Data Analytics. He has served as Leading Guest Editor for six special issues of IEEE, Elsevier, Springer and InderScience publications. He is an associate editor for IEEE Access and an Editor for the Elsevier Journal Internet of Things. His research interests include wearable sensing for smart health, machine learning for auxiliary diagnosis, and biomedical big data analytics.

Sarah Ali Siddiqui is a Chinese Government Scholarship holder with Shandong Provincial Key Laboratory of Network-Based Intelligent Computing, University of Jinan, China where she is currently a Computer Science Masters Degree student. She recieved her B.Sc in Electrical (Telecommunication) Engineering from COMSATS Institute of Information Technology, Islamabad, Pakistan. As the first author, she has published two peer reviewed journal papers in Elsevier and IEEE and as co-author, two peer reviewed papers in the IEEE conference proceedings. Her research interests are in mhealthcare and signal processing in healthcare domain.

Anton Kos received his Ph.D. in electrical engineering from the University of Ljubljana, Slovenia, in 2006. He is an assistant professor at the Faculty of Electrical Engineering, University of Ljubljana. He is a member of the Laboratory of Information Technologies at the Department of Communication and Information Technologies. His teaching and research work includes communication networks and protocols, quality of service, dataflow computing and applications, usage of inertial sensors in biofeedback systems and applications, signal processing, and information systems.He is the (co)author of more than thirty papers appearing in international engineering journals and of over fifty papers presented at international conferences.